JOURNAL OF PROPULSION AND POWER
Vol. 10, No. 2, March–April 1994

Combustion Zone—Acoustic Cavity Interactions in Rocket Combustors

Thomas L. Acker* and Charles E. Mitchell†
Colorado State University, Fort Collins, Colorado 80523

Analytical and numerical models are employed to assess the stabilizing impact of acoustic absorbers on liquid propellant rocket engine intrinsic stability. The tuning and stability behavior of cavities in which two-dimensional flow and temperature variations exist are predicted through the application of an iterative-integral, Green's function method of analysis. Results of stability calculations performed for a variety of cavity geometries and temperature gradients indicate that adding a large open area absorber to a combustion chamber significantly alters the spatial shape of the oscillation. This alteration consequently affects the driving and damping mechanisms in the chamber. Because of this interaction, the maximal stabilizing effect of a cavity with a given open area does not in general occur for a design tuned in the acoustic sense to the frequency of the oscillation, but rather for a design that is not tuned but which tends to maximize the influence of the damping mechanisms in the chamber relative to the driving mechanisms. Additionally, absorbers with large backing cavities are shown to perform better over a wider range of operating conditions than absorbers with small backing cavities. Calculations also reveal that large temperature gradients in an absorber tend to reduce its broadband effectiveness.

Nomenclature

F = nonhomogeneous part of main chamber governing equation
f = nonhomogeneous part of acoustic absorber governing equation
i = $\sqrt{-1}$, imaginary unit
L = main chamber length
L_A = total acoustic absorber length
L_c = acoustic absorber backing cavity length
l = integer
l_a = acoustic absorber aperture length
M_E = mean flow Mach number
m = integer
N = complex combustion response factor
n = integer or interaction index
$\boldsymbol{n}$ = outward unit normal vector
P = spatial component of main chamber pressure
p = spatial component of absorber pressure
R = acoustic absorber resistance
r = radial chamber dimension
r_c = main chamber radius
S = surface area
T = temperature
T_m = average temperature
t = time
u = mean axial main chamber velocity
V = volume
$\boldsymbol{V}$ = spatial part of main chamber velocity vector
$\boldsymbol{v}$ = spatial part of acoustic absorber velocity vector
W_c = acoustic absorber backing cavity width
w_a = acoustic absorber aperture width
X = acoustic absorber reactance
x, y = Cartesian coordinates used in the acoustic absorber analysis
Z_c = axial location where combustion is completed
z = axial chamber dimension
β = admittance function
Γ = empirical absorber resistance coefficient
γ = ratio of specific heats
δ = slope of linear temperature gradient
η = acoustic eigenvalue
θ = tangential chamber dimension
λ = imaginary part of ω, oscillatory decay/growth rate
μ = absorber backing cavity or main chamber coefficient matrix
ρ = mass density
ϕ = velocity potential
Ψ = velocity due to vorticity
Ω = acoustic eigenfunction
ω = complex oscillatory frequency
ω_R = real part of ω, actual oscillatory frequency

Superscripts

c = correction term
0 = lowest-order solution
$'$ = time dependent oscillatory component

I. Introduction

ACOUSTIC absorbers have been successfully employed in liquid-propellant rocket combustors to damp out acoustic instabilities.[1,2] Generally, it is accepted that acoustic resonators should operate close to their tuning frequencies in order to perform effectively.[3–6] For simple absorber geometries with no gas temperature variation, such as the quarter-wave tube and Helmholtz resonator, the acoustic tuning formulas are well understood. Predicting the overall stability enhancement caused by these devices, however, has been attained with only limited success.[7] This is due in part to previous analytical models not including all the chamber mechanisms influencing stability and their mutual interactions (i.e., mean flow, nozzle interactions, combustion, and absorbers). Furthermore, hardware considerations often require the construction of unconventional cavities such as the L-shape and T-shape absorbers (see Fig. 1), in which the flow is inherently two-dimensional (although Helmholtz resonators can be L- or T-shaped, many designs are not well modeled by the traditional mass-spring-damper analog employed in traditional Helmholtz resonator analysis). Also, since ab-

Received May 5, 1992; revision received Aug. 4, 1993; accepted for publication Sept. 3, 1993.

*Graduate Student, Department of Mechanical Engineering. Member AIAA.
†Professor, Department of Mechanical Engineering. Member AIAA.

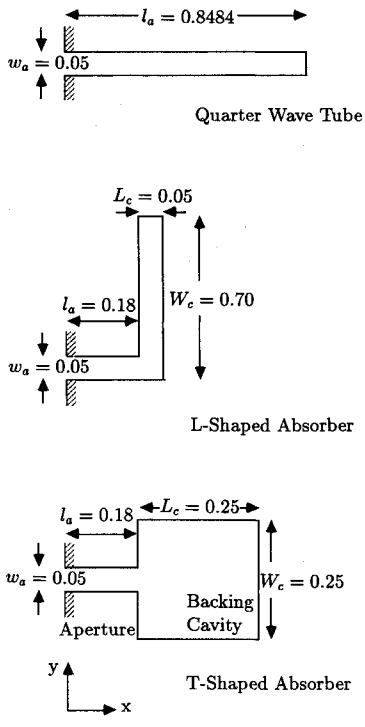

Fig. 1 Typical acoustic absorber geometries.

sorbers are located in the cooled chamber walls, large temperature profiles can exist in the gas filling the cavity.[8] Thus, a versatile and accurate model to predict cavity performance should include temperature variation for an arbitrary absorber geometry. Finally, to assess accurately the stabilizing impact of one of these devices, it is necessary to consider the influence of all the chamber mechanisms on stability.

The importance of stable rocket operation accompanied by high costs and lengthy development periods provides incentive to devise a predictive stability model to aid in the design of rocket combustors. Recent effort in stability modeling has resulted in computer codes capable of predicting the performance of acoustic absorbers used as stabilization devices.[9] Two main goals were accomplished in this work. An "open-loop" model to tune acoustically an absorber of arbitrary geometry with temperature variation was developed. The tuning model is referred to as open-loop because although the acoustic behavior of an absorber is determined, its impact on intrinsic chamber stability is not. This model was then included in a "closed-loop," linear stability model used to predict the stabilizing impact of an absorber considering combustion, mean flow, nozzle, and absorber interactions tied together in a feedback loop. The analytical approach employed in both the open-loop and closed-loop models involves the solution of a nonhomogeneous, linear wave equation by applying an iterative-integral, Green's function technique, subject to linear and nonlinear boundary conditions. Calculations were performed using the resultant stability code, final distributed oscillatory rocket combustion (FDORC). Specifically, the following questions were addressed:

1) How significantly will interaction among the chamber stability mechanisms affect the performance of an acoustic absorber?

2) How do temperature gradients affect the tuning and overall stability predictions of an absorber?

3) Do cavity gas temperature variations affect large-backing-cavity and small-backing-cavity absorbers equivalently?

II. Analysis

The same basic analytical technique is used to model the acoustic flowfield inside both the main chamber and the acoustic absorbers. The equations of motion are written down, nondimensionalized, and combined to form a single governing partial differential equation. Harmonic time dependency is assumed and the governing PDE is linearized. Applying an iterative-integral, Green's function technique to the particular geometry of interest, a solution is obtained. The main features of these solutions are presented in what follows.

A. Acoustic Absorber Modeling

The basic equations that apply to the acoustic flowfield are the conservation of mass, momentum, energy, and equations of state for a calorically perfect gas. Nondimensionalization of the equations is accomplished through division of the variables by the appropriate mean main chamber quantities evaluated at the location of the absorber entrance. All lengths are nondimensionalized by the main chamber radius; the main chamber mean sound speed is used to nondimensionalize velocity; the mean chamber pressure nondimensionalizes the absorber pressure; etc.

After nondimensionalization, the flow and state variables are separated into mean and oscillatory components. The basic equations are combined and a linearization is performed by assuming small amplitude oscillations and dropping all higher-order terms. Time dependency of the dependent variables is assumed to be harmonic, taking the exponential form $e^{i\omega t}$. For example, $P' = pe^{i\omega t}$, where $p = p(x, y)$ is the spatially-dependent part of the oscillatory pressure (refer to Fig. 1 for directions of x and y). After some manipulation, the following governing partial differential equation is obtained (see Ref. 10 for a detailed derivation):

$$\nabla^2 p + \frac{\omega^2}{\bar{T}} p = -\frac{1}{\bar{T}} \frac{d\bar{T}}{dx} \frac{dp}{dx} \tag{1}$$

where $\bar{T}$ is the local mean nondimensional value of T at a given cross section in the cavity. This mean temperature $\bar{T}$ is assumed to vary in an arbitrary way in the x direction. Thus, large temperature drops of up to 80% of the main chamber temperature can occur in the absorber. Velocity and pressure are related through the momentum equation by

$$v = \frac{i\bar{T}}{\gamma\omega} \nabla p \tag{2}$$

Equation (1) is subject to the boundary condition that the normal velocity be zero at the walls of the absorber.

To solve the governing partial differential equation (PDE), Eq. (1), a successive approximation, iterative-integral technique is employed. Absorber geometry is broken into two parts: 1) the aperture and 2) the backing cavity (see Fig. 1). Equation (1) is first solved considering two-dimensional flow in the backing cavity. Next, it is solved assuming one-dimensional flow in the aperture with the requirement that the velocity and pressure match at the aperture-cavity interface. A two-dimensional solution for the aperture as well has been performed in Ref. 10. For most geometries the impact of two-dimensional aperture effects was found to be small.

Due to the linearity of Eq. (1), the solution for p is broken into the sum of a lowest-order uniform-temperature solution plus a higher-order correction series to account for variable temperature effects. That is

$$p = p^0 + \sum_m \sum_n \mu_{mn} \Omega_{mn} = p^0 + p^c$$

where Ω_{mn} is the normalized eigenfunction of the region of interest (aperture or backing cavity), and μ_{mn} is the matrix of correction coefficients.

For the uniform-temperature solution, the right side of Eq. (1) becomes identically zero, and the lowest-order solution, p^0, is obtained via an eigenfunction expansion. Solution for the higher-order temperature correction term p^c, in both the

aperture and the backing cavity, is accomplished using a Green's function represented as an eigenfunction expansion. The resulting expression defining the correction coefficients is

$$\mu_{mn} = \frac{1}{(\omega^2/\bar{T}_m) - \eta_{mn}^2} \int_V \Omega_{mn} f(p, \bar{T})\, dV$$

where $f(p, \bar{T})$ is the right side of Eq. (1) and η_{mn} is the acoustic eigenvalue. Notice that to calculate μ_{mn}, a functional form of the pressure p is required. To lowest-order, p is represented by p^0. Once the μ_{mn} coefficients are determined, they are used to calculate the pressure correction term p^c. A new approximation of the pressure is then obtained using $p = p^0 + p^c$. Next, calculation of μ_{mn} is repeated with the current approximation of p. This process is repeated continually until successive computations of p are sufficiently invariant.

The performance of the absorber relative to the chamber oscillation is represented by the impedance which is defined as p'/u' evaluated at the absorber entrance plane. Since the velocity and pressure need not be in phase, the impedance is represented using complex notation, $p'/u' \equiv K \equiv R + iX$. The real part of the impedance is the resistance R, which is nonlinear as it accounts for the frictional dissipation of acoustic energy by gas jet formation at the cavity-chamber interface. The empirical formulation of the nonlinear resistance adopted in this analysis is $R = \Gamma\bar{\rho}u$ (nondimensional).[9] The imaginary part of the impedance is the reactance X, and is an indication of the phasing between the velocity and the pressure. Reactance is calculated by evaluating the ratio p/u at the absorber entrance [where p and u are the spatially-dependent parts of the oscillatory pressure and velocity as determined by solution of Eqs. (1) and (2)]. A detailed development of this analysis is presented by Dodd,[10] and also by Mitchell.[9,11]

B. Chamber Stability Model

Essentially the same basic equations are written down and nondimensionalized for the main chamber analysis as for the acoustic absorber analysis with the important difference that gas phase sources of mass, momentum, and energy must be included. The velocity field is separated into an irrotational part described through ϕ, and a rotational field Ψ, which appears because of the vorticity generated by the combustion sources, thus

$$V(r, \theta, z) = \nabla\phi(r, \theta, z) + \Psi(r, \theta, z) \tag{3}$$

Again, the dependent variables are represented as the sum of a mean and oscillatory component, and harmonic time dependency is assumed. The ratio of the local oscillatory mass generation rate $\dot{m}'$ to mean generation rate $\bar{\dot{m}}$ is represented by the product of the combustion response factor N with the local oscillatory pressure, $\dot{m}'/\bar{\dot{m}} = NP'$. The Crocco sensitive time lag theory[12] can be used to relate the combustion response factor to the complex frequency as follows:

$$N = n(1 - e^{-i\omega\tau})$$

where n is the interaction index relating the sensitivity of the combustion process to the pressure, and τ is the time lag which represents the delay time before the combustion process feels a pressure perturbation. The quantities n, τ (and thus N) are taken to be independent of location and time.

After combining the basic equations and applying the assumptions listed above, the partial differential equation for ϕ takes the following form:

$$\nabla^2\phi + \omega^2\phi = F\left(\phi, \frac{\partial\phi}{\partial z}, \bar{u}, \omega, \gamma, N\right) \tag{4}$$

This equation is derived in Ref. 13, where the expression for F is given in detail. The oscillatory pressure and rotational velocity Ψ are related to the oscillatory velocity potential ϕ by expressions of the form

$$P = P\left(\phi, \frac{\partial\phi}{\partial z}, \bar{u}, \frac{d\bar{u}}{dz}, \gamma\right)$$
$$\Psi = \Psi\left(\phi, \frac{\partial\phi}{\partial z}, \bar{u}, \frac{d\bar{u}}{dz}, N, \gamma\right) \tag{5}$$

Solving Eq. (4) subject to the boundary conditions imposed on the chamber, determines ϕ. Knowing ϕ, the oscillatory velocity and pressure fields are then given by Eqs. (3) and (5).

For a given mode of oscillation, Eq. (4) must satisfy oscillatory boundary conditions. The normal oscillatory velocity at the chamber walls is zero, $V\cdot n = 0$. At the chamber-absorber and chamber-nozzle interfaces, the normal oscillatory velocity will in general differ from zero, and is given by

$$V\cdot n = \beta P$$

In this expression, the admittance function β is defined as the ratio of oscillatory velocity to oscillatory pressure. To predict nozzle admittance, the analytical model developed by Bell and Zinn[14] is used, while the absorber admittance is predicted using the model given earlier.

Solution of the governing partial differential equation is once again obtained by using a successive approximation, Green's function technique. Transformation of Eq. (4) using Green's functions gives the following integral equation:

$$(\omega^2 - \eta_{K'}^2) \int_V \overline{\Omega_{K'}}\phi\, dV = \int_V \overline{\Omega_{K'}} F(\phi, \ldots)\, dV - \int_S \overline{\Omega_{K'}}(V\cdot n)\, dS \tag{6}$$

In this expression, ϕ is represented by a series summation of normalized eigenfunctions:

$$\phi = \sum_m \sum_l \sum_n \mu_{mln}\Omega_{mln}$$

where μ_{mln} is a matrix of correction coefficients, and Ω_{mln} is the normalized eigenfunctions with indices m, l, n. The eigenfunctions are found by solution of Eq. (4) for a closed cylindrical chamber ($F = 0$, $\nabla\phi\cdot n = 0$). $\overline{\Omega_{K'}}$ is the complex conjugate of the normalized eigenfunctions. The index $K' = m'l'n'$ indicates the specific harmonic component being analyzed in Eq. (6). Both standing and spinning tangential waves are possible along with radial and longitudinal modes and all forms of mixed modes. An iterative solution technique similar to the one described in the absorber analysis is used to solve for either the complex frequency or the combustion response. Note that the influences of the absorber and the nozzle on the chamber oscillation are accounted for in the surface integral shown in Eq. (5). During each iteration of the successive approximation solution technique, admittances are calculated at the current value of the main chamber frequency through implementation of the absorber and nozzle admittance models. Further details of the chamber stability analysis are given by Howell[15] and Mitchell.[9]

III. Results of Calculations

Though the number of possible acoustic absorber geometries is nearly limitless, two main groups can be identified as being typical practical designs: 1) absorbers with small backing cavities and 2) absorbers with large backing cavities. The quarterwave and L-shaped resonators shown in Fig. 1 are examples of small-backing-cavity absorbers, whereas the T-shaped absorber represents a large-backing-cavity absorber. In order to elucidate

the performance differences between the two groups of absorbers, both will be analyzed by performing open-loop reactance and closed-loop stability calculations.

A. Open-Loop Tuning Results

Generally, acoustic resonators are designed to remove a particular mode of oscillation. An absorber is considered tuned when its reactance is zero (i.e., at resonance). Knowing the mode (frequency) of oscillation, the reactance for an absorber of known geometry and gas conditions can be computed using the open-loop model described earlier. By varying either absorber geometry, gas conditions, or incident oscillatory frequency, while holding the other two fixed, a tuning curve can be generated which describes the sensitivity of the absorber to design or operation conditions. The effects on absorber reactance caused by mean temperature variations and changes in the incident frequency will be demonstrated by generating such tuning curves.

The effect of mean temperature variations on cavity reactance is displayed in Fig. 2 for the quarterwave and T-shaped resonators shown in Fig. 1. Curve 2 displays the reactance prediction for the quarterwave tube assuming a one-dimensional linear mean temperature profile given by $\bar{T}(x) = (1 + \delta x/L_A)$, where L_A is the total length of the resonator (aperture plus backing cavity $l_a + L_c$), x is the depth into the absorber, $\bar{T}$ is the temperature nondimensionalized with respect to the main chamber, and δ is the slope of the temperature gradient. Note that the reactance is zero at $\delta = 0$ (for the dimensions shown in Fig. 1, each absorber is tuned to the chamber first tangential ($1T$) mode, assuming the absorber gas temperature to be equal to the main chamber gas temperature). Curve 1 shows the calculated reactance for the same quarterwave tube as in curve 2, but assumes a constant gas temperature equal to the mean value given by the profile equation

$$\bar{T}_m = \left[\int \bar{T}(x)\, dx\right] \Big/ \int dx = 1 + \frac{\delta}{2}$$

Note that curves 1 and 2 lie nearly on top of one another except for large temperature variations ($\delta < -0.6$). This result indicates that an averaged mean temperature does a good job of predicting tuning lengths for moderate cavity gas temperature reductions. Curve 3 demonstrates the sensitivity of the large-backing-cavity T-shaped absorber to mean temperature variations. As shown, the slope of curve 3 is clearly less than that of curve 2, indicating the reactance of a quarterwave tube is more sensitive to temperature variations than the large-backing-cavity T-shaped absorber. In our calculations, this conclusion was found to be valid in general when comparing small-backing-cavity and large-backing-cavity absorbers. Similarly, it was also found that for mean temperature profiles different from linear, using the average cavity temperature did a good job of predicting tuning behavior, except for very large mean temperature decreases.

Another type of tuning curve is presented in Fig. 3. Here, absorber reactance is plotted vs the oscillatory frequency of an incident pressure wave for a cavity of fixed geometry and constant mean temperature (no variation with cavity depth). Curve 1 shows reactance variation for the previously described quarterwave tube tuned to the $1T$ mode, while curve 2 is for the large-backing-cavity T-shape tuned to the $1T$ mode by the two-dimensional analysis described earlier. Similar to the temperature variation results, the reactance of the quarterwave tube is more sensitive to frequency changes than the large-backing-cavity T-shaped absorber. Additional two-dimensional calculations indicate that this conclusion holds in general when comparing small-backing-cavity and large-backing-cavity absorbers of arbitrary design.

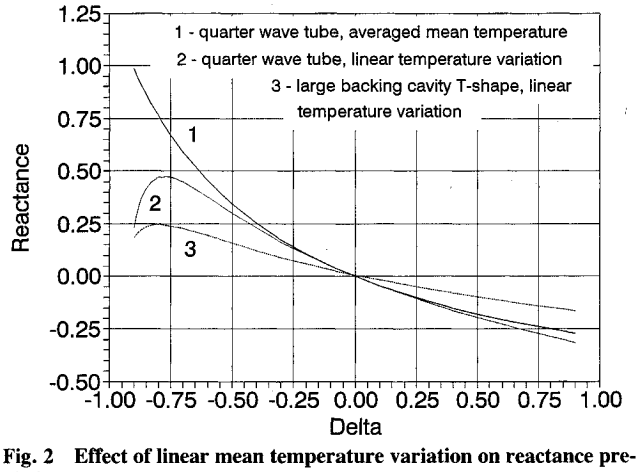

Fig. 2 Effect of linear mean temperature variation on reactance prediction.

B. Closed-Loop Chamber Stability Predictions

Conventional wisdom counsels that for maximum stabilizing impact on a chamber oscillation, an acoustic absorber should be tuned to the main frequency of interest. Moreover, increasing the open area (active area) of the absorber should also increase the damping produced by addition of the cavity. That this should be true for a chamber without combustion (or any other frequency sensitive driving or damping mechanism) seems clear. However, the fact that the combustion response to oscillations has been shown to be frequency sensitive, and that large open area cavities can serve to shift the frequency of the chamber oscillation, brings this simple guideline into question. In what follows, results of calculations are presented in which the open-loop model just described is combined with a chamber stability model which includes a frequency sensitive combustion response (n, τ model) in order to predict actual cavity damping performance in situ.

1. *Standard Chamber Configuration*

Before beginning an analysis of acoustic absorber influence on overall chamber intrinsic stability, it is necessary to define a standard combustion chamber configuration to which a given absorber will be added. Typical values for the cylindrical chamber length and combustion distribution were selected as $L = 2.5$ and $(Z_c/L) = 1.0$ (recall that all lengths are nondimensionalized with respect to the chamber radius). The ratio of specific heats of the combustion gases is assumed to be 1.2 with a mean flow Mach number of 0.2 at the convergent nozzle entrance. In an effort to isolate the effects of the absorber geometry and temperature on stability, the nozzle admittance is set equal to zero (no influence on oscillatory growth or decay; $\beta_N = 0 + i0$), and a uniform mean release of combustion product mass and energy is assumed. Though nozzle interactions, combustion distribution, and indeed, all

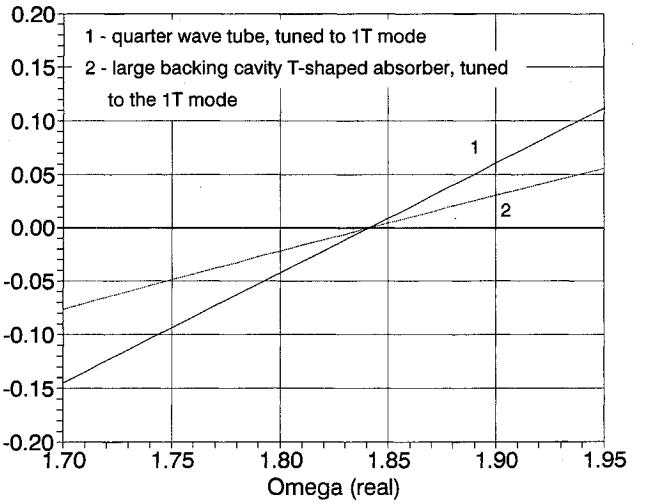

Fig. 3 Frequency-dependent tuning curves.

the chamber parameters just specified will affect chamber stability, the goal here is to compare the stability effects of different absorber geometries and cavity temperature profiles for a single simple chamber configuration. The effects of these several chamber design parameters and their interaction with cavity performance has been described elsewhere.[15] Since the maximum amplitude of a pressure wave in a combustor is generally located at the injector plate, thus providing the potential for maximum cavity interaction, each absorber investigated here will be located at the injector plate in the radial periphery of the chamber wall and will extend around the entire circumference of the chamber. The peak-to-peak oscillatory pressure amplitude is assumed to be 20% of the mean chamber pressure. Also, since the most damaging and likely oscillations are the low-order tangential modes, the chamber instability is assumed to be a spinning, 1T oscillation (unless otherwise stated).

As the first step in evaluating the impact of an acoustic absorber on the standard chamber's stability, its intrinsic stability in the absence of stabilization devices is examined. For neutrally stable oscillations in the 1T mode the minimum value of n required is predicted to be 0.915. The associated τ value is 1.675 (nondimensional). According to the sensitive time lag model, n and τ depend only upon the combustion process (injector, propellant combination, etc.). Thus, any propellant-injector combination supplying $n = 0.915$, $\tau = 1.675$ would be predicted to support neutrally stable 1T oscillations in the standard combustor. Because it is desirable to have a large stability margin, an absorber should be included on this chamber to ensure stable operation (damping of the 1T oscillation, $\lambda > 0$). Since these n, τ values represent the propellant-injector combination, they are unaffected by the addition of absorption devices. Thus, by adding an absorber to the standard chamber with n and τ fixed at 0.915 and 1.675, respectively, and determining its 1T stability using FDORC, the relative effectiveness of different absorbers can be ascertained by comparing their decay rates λ. Note that selection of these n, τ values is arbitrary and has been made for convenience in comparing the stability enhancement provided by different absorber designs. If, for instance, the propellant-injector combination of a combustion chamber were described by n, τ values which drove an intrinsically unstable 1T oscillation, all of the following results and conclusions would still apply. Indeed, the FDORC code was created so that a designer can take an intrinsically unstable chamber configuration and design an absorber which will cause stable operation.

The "open area" of an absorber is an additional parameter which is useful in comparing acoustic resonators. It is defined as the ratio of the entrance area to the absorber (chamber circumference multiplied by aperture width) to the area of the injector plate. For example, if an absorber is said to have a 10% open area, then this ratio equals 0.1. To compare fairly two different resonators, they should each have the same open area.

2. *In Situ Acoustic Absorber Design*

The primary motivation in developing our stability codes has been to include the interactions of combustion, mean flow, absorbers, and the nozzle in order to assess accurately the intrinsic chamber stability. It is possible to use this model to design the best performing absorber (providing the maximum decay of an incident pressure wave), while considering the absorber's interaction with the other chamber mechanisms. This "in situ" design process in conducted as follows. First, a general absorber geometry is decided upon which is consistent with the rocket engine configuration. Next, the resonator is tuned classically ($X = 0$) using the open-loop model and the acoustic frequency. This tuned absorber is then added to the chamber and the FDORC code is used to predict the complex oscillatory frequency, and thus the decay/growth rate of a particular mode of oscillation. Finally, by repeatedly varying an absorber dimension within FDORC (i.e., aperture length, backing cavity length or width) and calculating the associated damp rate, a design curve is traced out (damp rate vs absorber dimension). The optimal design is found at the peak of the curve. The following example will demonstrate the application of this technique.

Consider the standard chamber configuration defined earlier ($L = 2.5$, $Z_c/L = 1.0$, $\gamma = 1.2$, $M_E = 0.2$, $n = 0.915$, $\tau = 1.675$, $\beta_N = 0 + i0$). Classically tuning a 10% open area quarterwave tube to the frequency of a neutrally stable oscillation (1T mode) gives the following dimensions: $l_a = 0.8484$, $w_a = 0.05$ (assuming the gas temperature to be uniform and equal to the main chamber temperature). The decay rate of an oscillation will be given here as the percent decay per cycle of the chamber oscillation. Adding this cavity to the chamber (radially at the injector plate) will provide a predicted decay rate for the 1T traveling wave of 14.4% per cycle ($\lambda = 0.0442$). Recall that without the cavity the decay rate is zero. By varying the quarterwave-tube length l_a, and repeating the decay calculation, the design curve displayed as curve 1 in Fig. 4 is created. The asterisk on this curve denotes the decay rate of the oscillation using the tuned cavity. As shown, however, a maximum damp rate of nearly 40% per cycle ($\lambda = 0.150$) can be attained by employing a quarterwave tube of length $l_a = 0.745$. Even though the tuned absorber is at resonance and in phase with the chamber oscillation, the damp rate can be dramatically increased by using a shorter, untuned cavity. It is important to realize that this optimal absorber length is *not* the classical tuning length corresponding to the altered chamber frequency. The reactance of the optimal absorber in which maximum damping occurs is significantly different from zero. This behavior can be traced primarily to spatial pressure waveform modification caused by the strong interaction between the chamber mechanisms (combustion, absorber, and mean flow). Clearly, for this absorber, it is necessary to conduct an in situ analysis in order to determine optimal absorber geometry. An open-loop tuning approach is not adequate.

Curve 2 in Fig. 4 is an in situ design curve for a 4% open area quarterwave tube included on the standard chamber. The behavior is similar to the 10% open area results of curve 1, but with a reduced impact on stabilization. At the tuning length ($l_a = 0.8513$), the decay rate is 13.7% per cycle. By shortening l_a to 0.820, the damp rate is increased only slightly to 14.3%. Since the absorber open area is small, its influence on the pressure waveform is small, and only a modest increase in the decay rate is realized by performing an in situ analysis. The important conclusion to be drawn here is that for small open area absorbers, the usual method of designing resonators (by tuning) is adequate. However, for large open area absorbers (≥5%), it is necessary to conduct an in situ analysis to obtain the optimal cavity design. Note also that if the large open area absorber is not designed in situ, then the damping

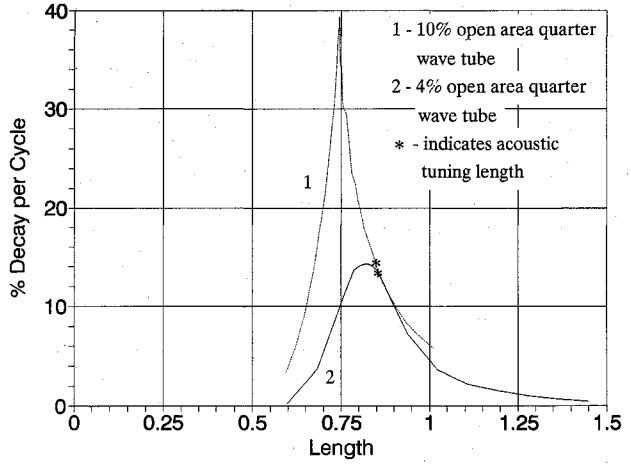

Fig. 4 In situ design curves for 4 and 10% open area quarterwave tubes.

it produces is only a meager one-half percent higher than for the small open area absorber.

To gain insight into how the interactions of the chamber mechanisms enable a detuned cavity to provide the maximum damping, it is helpful to examine the governing integral equation, Eq. (6). Damping provided by the absorber is accounted for in the absorber surface integral, and is approximately proportional to $P\beta_{L,\text{real}}$ where P is the average of the space dependent part of the oscillatory pressure ($P' = Pe^{i\omega t}$) at the absorber-chamber interface and $\beta_{L,\text{real}}$ is the real part of the absorber admittance (recall $\nabla\phi \cdot \boldsymbol{n} \equiv \beta P$). When an absorber is tuned, its $\beta_{L,\text{real}}$ is at a maximum. Classically, this means the absorber is dissipating acoustic energy with peak effectiveness, and therefore should provide the maximum damping. Fig. 5 shows $\beta_{L,\text{real}}$ for the 10% open area quarterwave tube plotted against cavity length divided by the optimal cavity length as determined by the in situ analysis. The peak of this curve corresponds to the tuned quarterwave tube length and shows $\beta_{L,\text{real}} \simeq 7.0$. For the optimally designed quarterwave tube which provides the maximum damping, however, $\beta_{L,\text{real}} \simeq 2.0$. However, since the damping goes as $P\beta_{L,\text{real}}$, the damp rates can be influenced significantly by different oscillatory pressure wave shapes and therefore different average pressures at the absorber. The axial pressure wave shapes along the chamber wall ($r = 1.0$, $\theta = 0$ deg) for the tuned and optimal absorber-chamber configurations are shown in Fig. 6. Since the pressure amplitude is arbitrary in this linear analysis, the curves in this figure are plotted by setting the pressure amplitude at the injector equal to 0.1 (nondimensional), and then calculating the pressure amplitude at all downstream locations relative to the amplitude at the injector. Curve 1 shows the pressure wave shape for the tuned absorber configuration. The influence of the tuned cavity is to drive down the oscillatory pressure amplitude at the absorber relative to the rest of the chamber. For the optimally designed absorber of curve 2, the effect on the chamber wave form is opposite; the oscillatory pressure amplitude at the absorber is large relative to the rest of the chamber.

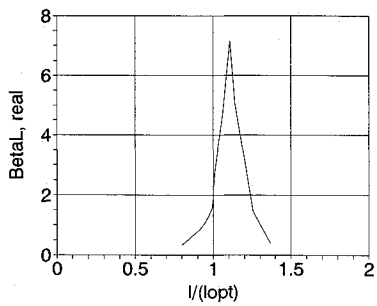

Fig. 5 Relationship between the real part of absorber admittance and optimal quarterwave tube length (10% open area).

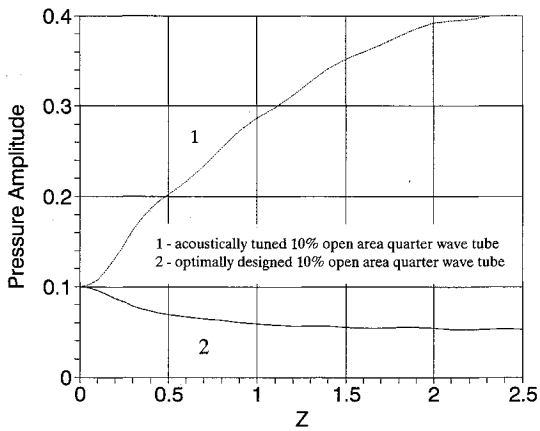

Fig. 6 1*T* axial pressure profile of the main chamber with a 10% open area quarterwave tube ($r = 1.0$, $\theta = 0.0$).

To compare justly how this waveform modification affects stability between the two different chamber-absorber configurations, it is necessary to examine the ratio of the absorber surface integral to the combustion—mean flow volume integral for each configuration. Since the nozzle on these chambers has no effect on stability ($\beta_N = 0$), the combustion, mean flow, and absorber are the only actors influencing the growth or decay of an oscillation. For the chamber with the optimally designed absorber, the ratio of the absorber surface integral to the combustion—mean flow volume integral is always larger than for the chamber with the tuned absorber. Physically, this implies in the chamber—tuned absorber configuration that though the cavity damping is high, the oscillatory pressure waveform is modified such that a relatively large amount of combustion driving still occurs. Antithetically, the chamber—optimal absorber configuration alters the wave shape such that a relatively smaller amount of combustion driving occurs, allowing the damping provided by the detuned absorber to dominate. Therefore, due to the complex interaction between the chamber and resonator, it is possible for an optimally designed, detuned absorber to provide the maximum possible oscillatory decay rate.

As alluded to earlier, the oscillatory decay rate of a small open area absorber can be increased only slightly by detuning the absorber according to an in situ analysis. It was therefore concluded that the absorber had only a small impact on the pressure waveform. This is displayed graphically in Fig. 7. Curve 1 shows the pressure waveform using the tuned 4% open area quarterwave tube, while curve 2 shows the wave shape employing the optimal resonator. As shown, the pressure amplitudes do not significantly vary throughout the

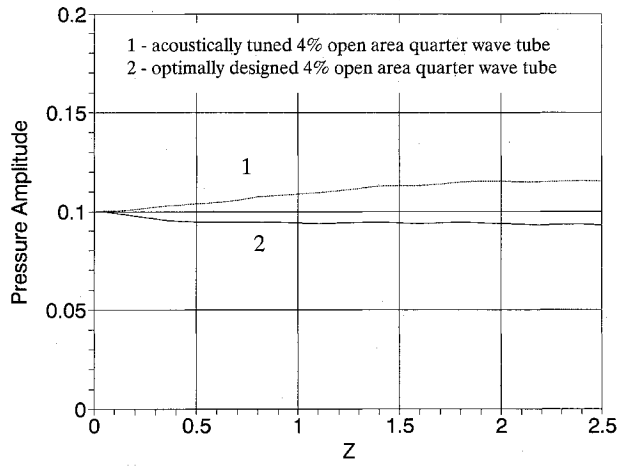

Fig. 7 1*T* axial pressure profile of the main chamber with a 4% open area quarterwave tube ($r = 1.0$, $\theta = 0.0$).

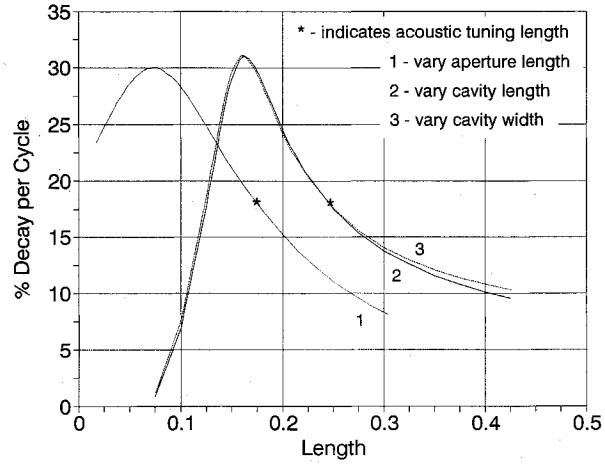

Fig. 8 In situ design curves for 10% open area large-backing-cavity T-shaped absorber.

chamber, nor do the shapes of the two curves differ drastically as in Fig. 8. This result reinforces the conclusion that an in situ analysis offers the greatest possibility for absorber design improvement in the case of large open area absorbers.

3. Geometrical Effects on Cavity Performance

Unlike the quarterwave tube, which for a given open area can be tuned only by varying its length, unconventional cavities such as the T-shape and L-shape offer three variable dimensions: l_a, L_c, and W_c. Thus, when optimally designing an absorber via the in situ analysis, any of these three dimensions can be varied. Figure 8 shows the in situ design curves for the large-backing-cavity T-shaped absorber attached to the standard chamber configuration. Curve 1 was created by varying l_a, while curves 2 and 3 were generated by changing L_c and W_c, respectively. In each case, the maximum decay achieved is around 31%, much greater than the tuned absorber decay of 17.5%. Curves 2 and 3 are also slightly thinner than curve 1. This is due to the larger volume change imposed by a change in a backing-cavity dimension as opposed to a change in the aperture length.

The results of the stability predictions just presented for two-dimensional cavities confirm those found in the quarterwave tube stability analysis. That is, for large open area absorbers, the classical tuning geometry is not nearly optimal due to the significant alteration of the chamber pressure waveform by the presence of the cavity. Therefore, to achieve maximum damping by the absorber, an in situ analysis should be performed. Also shown, for an unconventionally shaped resonator which has three variable design dimensions (l_a, W_c, L_c), essentially the same maximum damp rate is found regardless of which dimension is varied. In every case, the optimally designed absorber exhibits a decrease in volume from the classical tuning point. Additional calculations performed for a variety of cavity shapes, including geometries with small backing volumes, have shown the same types of behavior as the quarterwave tube and the T-shaped resonators.

4. Temperature Effects on Cavity Performance

The open-loop results presented earlier indicated that mean temperature gradients in acoustic cavities significantly affected their reactance. The impact of temperature variations on the performance of acoustic cavities measured in terms of overall decay rate produced has been assessed using the stability model. In the first series of calculations to be presented, the effect of temperature gradients on in situ design curves was evaluated.

Results of these calculations are shown in Fig. 9. Curve 1 in this figure is the design curve for a large-backing-volume T-shaped absorber. The curve presents the same results as curve 1 of Fig. 8 (uniform mean temperature), except that in Fig. 9 the decay rate is plotted vs l_a divided by the aperture length for acoustic tuning. As displayed on curve 1, a maximum damp rate of slightly more than 30% is obtained by reducing the aperture length to less than 40% of its tuned size. Assuming a linear decrease in absorber gas temperature down to half of the mean chamber gas temperature, the absorber's tuned backing cavity length was found using the open-loop model to be 21% shorter than with no temperature variation (all other resonator dimensions being the same as for no temperature variation). The result of performing an in situ analysis of this variable temperature cavity by changing the aperture length is shown as curve 2 of this figure. An increase in damping per cycle from 16.5 to 31% is realized by decreasing l_a by about 50%. For a large variation in absorber temperature down to 20% of the mean chamber temperature, the tuned backing cavity length is 25% shorter than with no temperature variation. Curve 3 displays the in situ design curve for this absorber-chamber configuration by once again varying l_a. The maximum decay rate of 32% per cycle is produced when the aperture length is reduced by just over 40%. Comparing the three curves, it is evident that as the absorber gas temperature decreases, the design curves become steeper with a slightly higher peak. The increased steepness is due to the fact that the absorber reactance varies more rapidly with geometrical changes for larger cavity gas temperature gradients. Consequently, the change in length between the tuned cavity and the optimal cavity becomes smaller as the reduction in absorber gas temperature increases. Since the geometry of a resonator designed optimally at a relatively lower temperature is closer to its tuned geometry than an optimal cavity designed at a relatively higher temperature, it is able to provide a slightly higher decay rate ($\beta_{L,\text{real}}$ increases by a small amount). These results indicate clearly that it is important to include temperature variation when designing a large-backing-cavity acoustic absorber for optimal stabilizing impact.

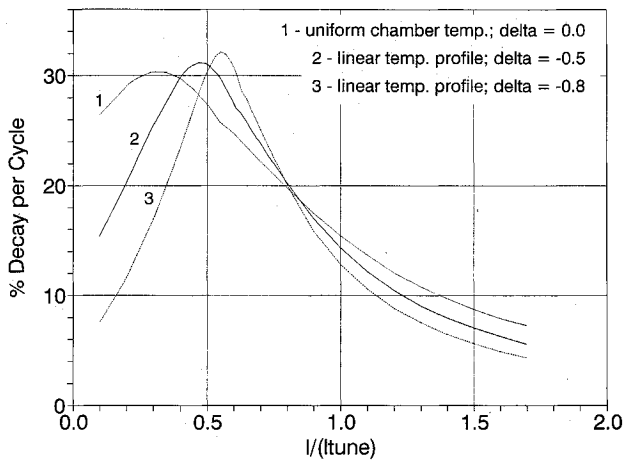

Fig. 9 Temperature effect on in situ design curves for a large-backing-cavity T-shaped absorber.

In practice, it is difficult to distinguish accurately the shape of an absorber's gas temperature variation. A designer, therefore, would be interested in knowing how a given absorber will perform under off-design temperature conditions. As will be demonstrated, optimally designed cavities (designed using the in situ technique) perform well over a wide temperature range, much better than their corresponding tuned cavities (designed using the open-loop technique). Additionally, large-backing-cavity absorbers will be shown to operate more effectively at off-design temperatures than small-backing-cavity absorbers. To investigate the off-design behavior, the large-backing-cavity T-shaped absorbers optimally designed to the 1T mode on the standard chamber (see Fig. 9) were evaluated using FDORC while varying the absorber temperature profile.

The optimally designed 10% open area large-backing-cavity T-shaped absorber with no temperature variation was found to provide a 1T damp rate of 30% per cycle. Recall that the slope of a linear temperature gradient is characterized by δ: $\bar{T}(x) = \bar{T}(x = 0)[1 + \delta x/L_A]$. Thus, by varying δ in a fixed absorber geometry from 0 to -0.8, the damp rate can be calculated for linear temperature drops in the cavity from zero (uniform temperature equal to the chamber temperature; $\delta = 0$), down to 20% of the mean chamber temperature ($\delta = -0.8$). The resulting decay rates can then be plotted vs δ to display the temperature "bandwidth" of the resonator. Carrying out this procedure for the uniform temperature absorber previously described results in curve 1 of Fig. 10. As displayed, the maximum damping provided by this absorber occurs at the design temperature condition ($\delta = 0$), and gradually decreases with the gas temperature. The curving up at the low temperature end of the curve is explained by referring to open-loop tuning curve 3 in Fig. 2. The important conclusion is that an optimally designed cavity will perform well at off-design temperature conditions. Curves 2 and 3 in Fig. 10 plot the temperature bandwidths of absorbers optimally designed assuming temperature gradients of $\delta = -0.5$ and δ

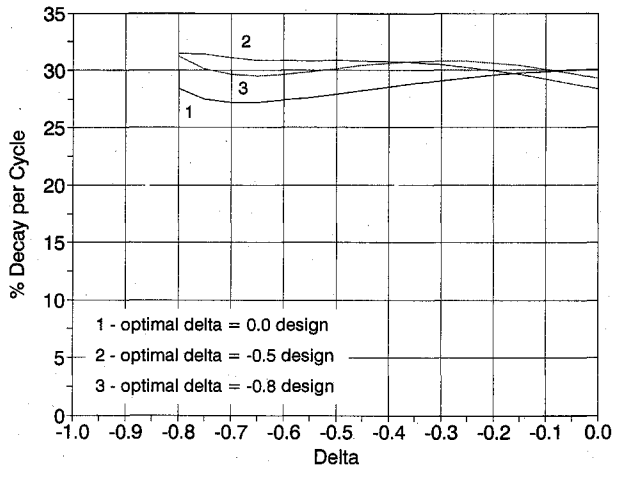

Fig. 10 Off-design temperature performance of large-backing-cavity T-shaped absorbers optimally designed with linear temperature variation.

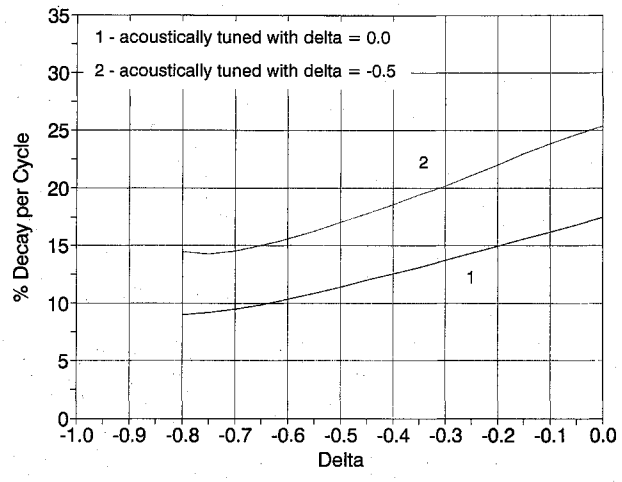

Fig. 11 Off-design temperature performance of acoustically tuned large-backing-cavity T-shaped absorbers.

$= -0.8$, respectively. Again, both of these resonators perform well, providing a "wide" temperature bandwidth. Taken together, the results shown in Fig. 10 indicate that regardless of the assumption made about the temperature profile in the T-shaped cavity, optimally designed cavities (using the in situ method) work very well whatever the form of the actual temperature gradient.

Considering the limited success in predicting tuned absorber damping in the past (i.e., absorbers designed using the open-loop method), it is of interest to look at their performance under off-design temperature conditions. A 10% open area large-backing-cavity T-shaped absorber tuned considering no temperature variation will provide a $1T$ decay rate of about 17% per cycle. Varying the temperature in the absorber and recalculating the damp rate generates curve 1 in Fig. 11. As displayed, the decay rate of this absorber drops off from its tuned value as the temperature decreases. Curve 2 displays the temperature bandwidth of a similar large-backing-cavity T-shape tuned with a moderate temperature gradient, $\delta = -0.5$, and having an on-design damp rate of also 17% per cycle. Note that while the damp rate of this resonator decreases for lower gas temperatures, it actually increases for higher gas temperatures. This increase occurs because the tuned length of the $\delta = -0.5$ absorber is relatively short, and thus for higher temperatures its length becomes closer to the optimal length (as determined by in situ calculations) causing the damp rate to go up. As shown, if employing a tuned absorber, the oscillatory decay provided can vary substantially depending on the gas temperature. This contrasts with the modest dependence exhibited by optimal cavities. Also, the decay provided will generally be much less than provided by an optimally designed absorber.

Large-backing-cavity and small-backing-cavity absorbers of equal open area tend to provide similar damp rates when designed optimally. In the open-loop tuning results, however, it was concluded that the reactance of small-backing-cavity absorbers was more sensitive to changes in temperature than large-backing-cavity absorbers. Thus, one might expect the temperature bandwidth of small-backing-cavity absorbers to be "thinner" than for large-backing-cavity absorbers (near optimal over a smaller temperature range). This behavior is displayed in Fig. 12. Curve 1 was generated for the 10% open area small-backing-cavity L-shaped absorber shown in Fig. 1, when optimally designed to the $1T$ mode with no gas temperature variation. Maximum damping is provided by the absorber at its design temperature ($\delta = 0$), but rapidly declines as the gas temperature decreases. Curve 2 exhibits a similar behavior for a small-backing-cavity L-shape optimally sized assuming $\delta = -0.5$. The damping provided by this resonator also peaks at its design temperature and quickly decreases at off-design temperatures. Comparing the average decay rate over the entire temperature range of the small-backing-cavity L-shape to the large-backing-cavity T-shape, it is evident that the large-backing-cavity T-shaped resonator performs better at off-design temperatures. Additional calculations indicate that this conclusion holds in general when comparing large-backing-cavity and small-backing-cavity absorbers.

Several important conclusions have been drawn from these temperature bandwidth results. Large-backing-cavity absorbers designed using the in situ technique provide near optimal damping over a very broad mean cavity temperature range. In contrast to this, a tuned cavity designed using the open-loop technique, regardless of its gas temperature profile, does not maintain its damping impact at off-design temperatures. These results suggest a method to design confidently resonators that will provide near optimal damping if uncertain of the absorber temperature profile: optimally design an absorber with a large backing cavity using the in situ technique.

5. *Design Considerations at Higher Modes of Oscillation*

The results previously presented addressed the effects of temperature gradients and two-dimensional flow (unconventional shapes) on acoustic absorber performance when subjected to a $1T$ traveling wave in the standard chamber configuration. Several conclusions were drawn suggesting an optimal in situ design process in order to maximize the damping provided by a given absorber. Similar results have been obtained for other modes of oscillation (e.g., $2T$, $3T$, $1R$), leading to the same conclusions about the interaction between

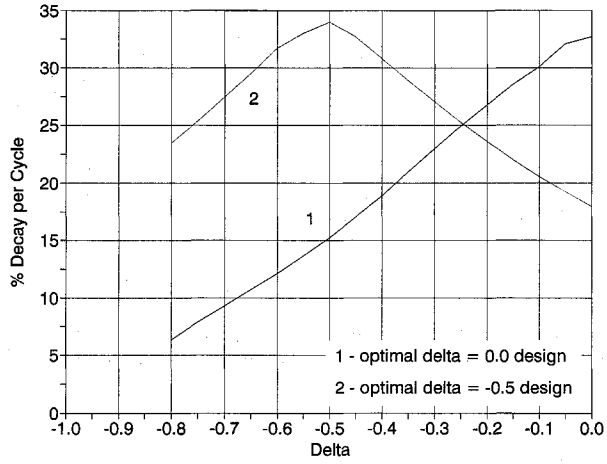

Fig. 12 Off-design temperature performance of small-backing-cavity L-shaped absorbers optimally designed with linear temperature variation.

the chamber stability mechanisms and the need for in situ absorber design. For more details about the prediction of cavity performance at other modes of oscillation and also at off-design modes of oscillation, the reader is encouraged to consult Ref. 9.

IV. Conclusions

The purpose of this study was to use a comprehensive linear stability model to gain insight into the complex absorber-chamber interaction found in rocket engines, and to investigate the effects of two-dimensional flow and temperature variation on acoustic absorber performance and design. The results presented show that addition of a large open area absorber ($\geq$5% of the injector plate area) to a chamber will significantly alter the shape of the main chamber oscillatory pressure wave. Due to this effect, detuned absorbers optimally designed to remove a specific mode of oscillation using an in situ analysis are found to provide the maximum damping. The optimal absorber, which exhibits a decrease in volume from the acoustically tuned absorber, provides maximum decay rates because the chamber waveform is altered favorably such that the cavity damping dominates the combustion driving to a greater extent than is the case for an acoustically tuned cavity. Optimally designed large open area absorbers can provide over twice the damping of acoustically tuned absorbers with the same open area. Additionally, large-backing-cavity absorbers designed using the in situ technique maintain near optimal damping over a wider range of cavity gas temperatures than small-backing-cavity absorbers. This effect is due to the greater sensitivity of small-backing-cavity absorbers to variations in temperature and frequency, as demonstrated by open-loop reactance calculations. Though best results are achieved by optimal in situ design knowing the exact size of the gas temperature variation, these conclusions suggest a convenient method to design confidently an absorber that will perform well over a wide range of temperatures: assume a moderate average cavity gas temperature and conduct and optimal in situ design of a large-backing-cavity absorber.

Acknowledgments

This research was sponsored in part by the Air Force Phillips Laboratory, Edwards Air Force Base, California, under Contract FO4611-86-k-0020.

References

[1]Coultas, T. A., Oberg, C. L., and Senneff, J. M., *Liquid Propellant Rocket Combustion Instability*, edited by D. T. Harrje and F. H. Reardon, NASA SP-194, 1972, Chap. 8.3.6, pp. 426–429.

[2]Oberg, C. L., "Combustion Stabilization with Acoustic Cavities," *Journal of Spacecraft and Rockets*, Vol. 8, No. 12, 1971, pp. 1220–1226.

[3]Tang, P. K., and Sirignano, W. A., "Theoretical Studies of a Quarter-Wave Tube," AIAA Paper 71-87, Jan. 1971.

[4]Tang, P. K., and Sirignano, W. A., "Theory of a Generalized Helmholtz Resonator," *Journal of Sound and Vibration*, Vol. 26, No. 2, 1973, pp. 247–262.

[5]Oberg, C. L., Wong, T. L., and Ford, W. M., "Evaluation of Acoustic Cavities for Combustion Stabilization," 7th JANNAF Combustion Meeting, Oct. 1971.

[6]Phillips, B., Hannum, N. P., and Russel, L. M., "On the Design of Acoustic Liners for Rocket Engines: Helmholtz Resonators Evaluated with a Rocket Combustor," NASA TN D-5171, April 1969.

[7]Oberg, C. L., and Wong, T. L., "Combustion Instability Suppression Devices," 8th JANNAF Combustion Meeting, CPIA Pub. 220, Vol. 1, 1971, pp. 781–794.

[8]Oberg, C. L., Wong, T. L., and Ford, W. M., "Final Report: Evaluation of Acoustic Cavities for Combustion Stabilization," NASA CR-115087, July 1972.

[9]Mitchell, C. E., "Final Report: Stability Design Methodology," Edwards AFB, CA, Final Report on Air Force Contract FO4611-86-K0020, AF-TR-89-041, Vols. 1 & 2, 1989.

[10]Dodd, F. E., "Two Dimensional and Temperature Effects on Acoustic Cavity Performance in Rocket Engines," M.S. Thesis, Dept. of Mechanical Engineering, Colorado State Univ., Fort Collins, CO, Summer 1988.

[11]Mitchell, C. E., Dodd, F. E., Acker, T. L., and Howell, D. J., "Two Dimensional and Temperature Effects on Acoustic Cavity Tuning and Performance in Rocket Combustors," *Proceedings of the Winter Annual Meeting of the American Society of Mechanical Engineers*, NCA—Vol. 4, HTD—Vol. 128, 1989, pp. 11–16.

[12]Crooco, L., *Liquid Propellant Rocket Combustion Instability*, edited by D. T. Harrje and F. H. Reardon, NASA SP-194, 1972, Chap. 4.2, pp. 170–194.

[13]Mitchell, C. E., "Improvement of an Integral Stability Model," 22nd JANNAF Combustion Meeting, CPIA Pub. 432, Vol. 1, 1985, pp. 443–452.

[14]Bell, W. A., and Zinn, B. T., "The Prediction of Three Dimensional Liquid Propellant Rocket Nozzle Admittances," NASA CR-121129, Feb. 1983.

[15]Howell, D. J., "Three Dimensional Linear Acoustic Stability Models for Rectangular and Cylindrical Rocket Combustors," M.S. Thesis, Dept. of Mechanical Engineering, Colorado State Univ., Fort Collins, CO, Summer 1989.